

Vibration and impedance monitoring for prestress-loss prediction in PSC girder bridges

Jeong-Tae Kim*, Jae-Hyung Park‡, Dong-Soo Hong‡, Hyun-Man Cho†† and Won-Bae Na††

Department of Ocean Engineering, Pukyong National University, Busan, Korea

Jin-Hak Yi†††

Korea Ocean Research & Development Institute, Ansan, Korea

(Received November 7, 2007, Accepted July 30, 2008)

Abstract. A vibration-impedance-based monitoring method is proposed to predict the loss of prestress forces in prestressed concrete (PSC) girder bridges. Firstly, a global damage alarming algorithm using the change in frequency responses is formulated to detect the occurrence of damage in PSC girders. Secondly, a local damage detection algorithm using the change in electro-mechanical impedance features is selected to identify the prestress-loss in tendon and anchoring members. Thirdly, a prestress-loss prediction algorithm using the change in natural frequencies is selected to estimate the extent of prestress-loss in PSC girders. Finally, the feasibility of the proposed method is experimentally evaluated on a scaled PSC girder model for which acceleration responses and electro-mechanical impedances were measured for several damage scenarios of prestress-loss.

Keywords: structural health monitoring; prestress-loss; vibration-based damage detection; PSC girder; vibration; electro-mechanical impedance; modal parameters.

1. Introduction

Recently, the interest on structural health monitoring of prestressed concrete (PSC) girder bridges has been increased. For a PSC girder bridge, the prestress force in tendon is an important parameter that should be secured for its serviceability and safety against external loadings and environmental conditions (Lin 1963, Nawy 1996). The loss of the tendon's prestress force (hereafter, prestress-loss) occurs along the entire girder due to elastic shortening and bending of concrete, creep and shrinkage of concrete, steel relaxation and frictional loss, and damage or severing of prestress strands.

Unless the PSC girder bridges are instrumented at the time of construction, the occurrence of damage cannot be directly monitored and other alternative methods should be sought. Since as early as 1970s, many researchers have focused on the possibility of using vibration characteristics of a structure as an

*Professor, E-mail: idis@pknu.ac.kr

‡Ph.D. Candidate

‡‡BK21 Assistant Professor

‡‡‡Assistant Professor

‡‡‡‡Senior Research Scientist

indication of its structural damage (Adams, *et al.* 1978, Stubbs and Osegueda 1990, Kim and Stubbs, 1995, Doebling, *et al.* 1998, Kim, *et al.* 2003a). Recently, research efforts have been made to monitor the change in modal properties in related to the change in prestress forces (Saiidi, *et al.* 1994, Saiidi, *et al.* 1996), to investigate the dynamic behaviors of prestressed composite girder bridges (Miyamoto, *et al.* 2000), and to identify the change in prestress forces by measuring dynamic responses of prestressed beams (Kim, *et al.* 2003b, Law and Lu 2005).

Based on the previous works, however, the physical type of local damage can not be easily identified via vibration-based approaches unless the information on real damage is known. Recently, electro-mechanical impedance-based health monitoring has shown the promising success to detect minor changes in structural integrity (Park, *et al.* 2000, Bhalla and Soh 2003, Giurgiutiu and Zagari 2005). Compared to vibration-based approaches, the impedance-based method has the capability of more accurately locating damage such as cracks on small scale. To-date, research attempts have been made to extensively investigate the applicability of the impedance technique on a scaled bridge element (Park, *et al.* 2000), to verify the feasibility of the technique for detecting the change in structural integrity of a model reinforced concrete frame (Bhalla and Soh 2003), to identify the change in support conditions simulated in a model plate-girder bridge by using the change in impedance signatures (Kim, *et al.* 2006), to long-term monitor post-tensioned tendons by using direct capacitance and resistance measurements (Elsener 2005), to monitor cracks incurred in a reinforced concrete beam by using the change in impedance signatures (Park, *et al.* 2006b) and to estimate the sensitivity and the sensing region of the PZT sensor in concrete structures (Yang, *et al.* 2008).

In this paper, a vibration-impedance-based monitoring method is proposed to predict the loss of prestress forces in prestressed concrete (PSC) girder bridges. To achieve the objective, the following approaches are implemented. Firstly, a global damage alarming algorithm using the change in frequency responses is newly formulated to monitor the occurrence of damage in PSC girders. Secondly, a local damage detection algorithm using the change in electro-mechanical impedance features is selected to identify the prestress-loss in tendon and anchoring members. Thirdly, a prestress-loss prediction algorithm using the change in natural frequencies is selected to estimate the extent of prestress-loss in PSC girders. Finally, the feasibility of the proposed method is experimentally evaluated on a scaled PSC girder model for which acceleration responses and electro-mechanical impedance signatures were measured for several damage scenarios of prestress-loss.

2. Prestress-loss monitoring methods

A vibration-impedance-based scheme for monitoring prestress-loss is designed as follows: 1) Alarming the occurrence of damage in PSC girder by globally monitoring the change in frequency response functions, 2) Identifying the alarmed damage as prestress-loss in tendon and anchoring members by locally monitoring the change in electro-mechanical impedances, and 3) Estimating the extent of the alarmed damage by using a frequency-based method proposed by Kim, *et al.* (2003b).

2.1. Global damage alarming method using frequency response functions

Damage occurrence may be detected using frequency response of the structure. The basic idea is that frequency responses are functions of the structural properties such as mass, damping and stiffness. Damage causes the change in structural properties, which, in turn, results in the change in frequency responses of the structure.

For the relationship between the input force and the output response of a structural system, the frequency response function, $H(f)$, is defined as follows (Bendat and Piersol 1993):

$$H(f) = \frac{V(f)}{U(f)} = \frac{1}{-m(2\pi f)^2 + ic(2\pi f) + k} \quad (1)$$

where $U(f)$ and $V(f)$ are, respectively, force and displacement transformed into frequency domain. Also, m , c and k are, respectively, mass, damping and stiffness of the structural system.

On assuming a harmonic force, $U_j(\omega_k)$, is excited with the k th natural frequency ω_k and is applied at m locations ($j = 1, \dots, m$) at the same time, then the displacement ratio between two outputs at locations i and $i+1$ is given as follows:

$$\frac{V_i(\omega_k)}{V_{i+1}(\omega_k)} = \frac{\sum_{j=1}^m H_{i,j}(\omega_k) U_j(\omega_k)}{\sum_{j=1}^m H_{i+1,j}(\omega_k) U_j(\omega_k)} = \frac{H_i(\omega_k)}{H_{i+1}(\omega_k)} \quad (2)$$

Furthermore, a frequency-response-ratio (FRR) function between the locations i and $i+1$ is defined as

$$FRR_{i,i+1}(\omega_k) = \frac{S_{i,i}(\omega_k)}{S_{i,i+1}(\omega_k)} = \frac{E[V_i^*(\omega_k)V_i(\omega_k)]}{E[V_{i+1}^*(\omega_k)V_{i+1}(\omega_k)]} = \frac{H_i(\omega_k)}{H_{i+1}(\omega_k)} \quad (3)$$

where $S_{i,i+1}(\omega_k)$, $S_{i,i}(\omega_k)$ are cross-spectral and auto-spectral density functions, respectively. By comparing a frequency-response-ratio measured at an undamaged baseline state to the corresponding one at a subsequent damaged state, a frequency-response-ratio assurance criterion ($FRRAC$) can be defined as follows:

$$FRRAC(b, d) = \frac{\{FRR_b^T FRR_d\}^2}{\{FRR_b^T FRR_d\} \{FRR_b^T FRR_d\}} \quad (4)$$

where the subscripts b and d denote the undamaged baseline state and its corresponding damaged state, respectively. Eq. (4) represents the linear relationship between the pre-damaged frequency-response-ratio, FRR_b , and the post-damage frequency-response ratio, FRR_d . The $FRRAC$ remains close to 1.0 if no damage. Otherwise, the $FRRAC$ decreases from 1.0 if damage occurred (i.e. changes in physical properties m , c and k).

2.2. Local damage identification method using impedance signatures

Impedance-based health monitoring techniques utilize piezoelectric materials as sensors and actuators. When a piezoelectric material is mechanically strained, an electrical field is produced. Conversely, its shape is changed when an electrical field is applied. In addition, the materials have unique structures, which allow bidirectional coupling between electric field and strain; hence, they are useful for self-sensing, power harvesting, and SHM applications (Liang, *et al.* 1996, Kabeya 1998, Park, *et al.* 2000, Giurgiutiu and Zagrai 2005, Bhalla and Soh 2003, Yang, *et al.* 2005, Park, *et al.* 2006a, Park, *et al.* 2006b).

As shown in Fig. 1, the active material is described by its short circuited mechanical impedance, which is powered by voltage or current. The host structure is modeled as the effect of mass, stiffness, damping,

and boundary conditions. For a SDOF system, the mechanical impedance of the host structure, $Z_s(\omega)$, is defined as the ratio of a harmonic excitation force F_o at the angular frequency ω to the velocity response \dot{v} in frequency domain:

$$Z_s(\omega) = \frac{F_o}{\dot{v}} = |Z_s(\omega)|e^{i\theta} \quad (5a)$$

in which

$$|Z_s(\omega)| = \sqrt{c^2 + \frac{(m\omega^2 - k)^2}{\omega^2}}, \theta = \tan^{-1} \frac{m\omega^2 - k}{c\omega} \quad (5b)$$

In Fig. 1, the piezoelectric material is considered as a thin bar undergoing axial vibration. When a piezoelectric patch is surface-bonded to a structure, the electrical admittance (the inverse of electro-mechanical impedance) of the patch, $Y(\omega)$, is a combined function of the mechanical impedance of the host structure, $Z_s(\omega)$, and that of the piezoelectric patch, $Z_a(\omega)$ (Liang, *et al.* 1994):

$$Y(\omega) = i\omega \frac{wl}{t_c} \left[(\varepsilon_{33}^T - d_{3x}^2 \hat{Y}_{xx}^E) + \frac{Z_a(\omega)}{Z_a(\omega) + Z_s(\omega)} d_{3x}^2 \hat{Y}_{xx}^E \left(\frac{\tan kl}{kl} \right) \right] \quad (6)$$

where \hat{Y}_{xx}^E is the complex Young's modulus of the at zero electric field; ε_{33}^T is the dielectric constant of piezoelectric wafer; d_{3x} is the piezoelectric coupling constant in the x direction at zero stress; k is the wave number that depends on mass density and Young's modulus of the piezoelectric material; and w , l , and t_c are, respectively, the width, length, and thickness of the piezoelectric transducer.

This equation indicates that the electrical impedance of the piezoelectric patch bonded onto a host structure is directly related to the mechanical impedance of the structure. The first term of the equation is the capacitive admittance of the free piezoelectric patch. The second term includes the mechanical impedance of both the piezoelectric patch and the host structure. As described in Eq. (6), when damage occurs to a structure, its mechanical impedance will be changed. Hence, any changes in the electrical impedance signature (such as magnitude of admittance and frequency) are attributed to damage or changes in the structure. However, it is also noted that piezoelectric materials have temperature dependent properties, then environmental effects other than damage may cause some drifts in the electrical impedance signatures.

The complex admittance $Y(\omega)$ (units Siemens or ohm^{-1}) consists of real and imaginary parts, which are the conductance (G) and the susceptance (B), respectively. These can be measured by commercially

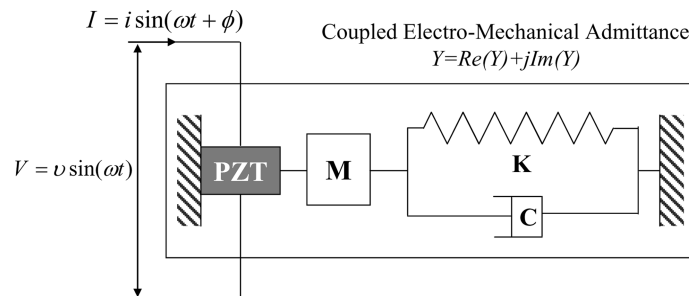


Fig. 1 1-D Model of electro-mechanical interaction of piezoelectric patch and host structure (Liang, *et al.* 1994)

available impedance analyzers. To enhance the sensitivity to incipient damage, the electrical impedance is usually measured at high frequencies, at which the wavelengths of the structural vibration are shorter than the damage to be detected. In general, high frequency (ranged 30 to 300 kHz) low voltage (less than 1V) structural excitations are used to monitor the electrical impedance of the piezoelectric patch.

2.3. Prestress-loss estimation method using modal parameters (Kim, et al. 2003b)

Kim, et al. (2003b) proposed an equivalent flexural rigidity model as schematized in Fig. 2. Consider a simply-supported, uniform cross-sectional, PSC beam with a straight concentric tendon. Suppose that the beam is in axial compression due to the prestress loads applied at the anchorage edges. Then we can model that the beam is initially deformed in compression up to the deformed span length L_r (i.e. reduced in span length by δL) and the tendon is still in tension due to the constraint (i.e. anchoring) after elastic stretching for prestressing effect. The governing differential equation for the beam is expressed by:

$$\frac{\partial^2}{\partial x^2} \left(E_r I_r \frac{\partial^2 y}{\partial x^2} \right) + m_r \frac{\partial^2 y}{\partial t^2} = 0 \quad (7)$$

where $E_r I_r (= E_c I_c + E_s I_s)$ represents composite flexural rigidity of PSC beam section, in which $E_c I_c$ is flexural rigidity of concrete beam-section and $E_s I_s$ is equivalent flexural rigidity corresponding to the contribution of the tendon on the flexural resistance. Also, $m_r (= \rho_c A_c + \rho_s A_s)$ is the mass per unit length of PSC beam that combines the mass of concrete beam, $\rho_c A_c$, and the mass of the tendon, $\rho_s A_s$.

By equating modal characteristics of a cable under tension load N to those of a beam with equivalent flexural stiffness, the equivalent flexural rigidity of tendon is derived as follows (Kim, et al. 2003b):

$$E_s I_s = \left(\frac{L_r}{n\pi} \right)^2 N \quad (8)$$

Applying Eq. (8) and appropriate boundary conditions to Eq. (7) leads the n th natural frequency, ω_n , of the residual-tension model as follows:

$$\omega_n^2 = \left(\frac{n\pi}{L_r} \right)^4 \frac{1}{m_r} \left(E_c I_c + \left(\frac{L_r}{n\pi} \right)^2 N \right) \quad (9)$$

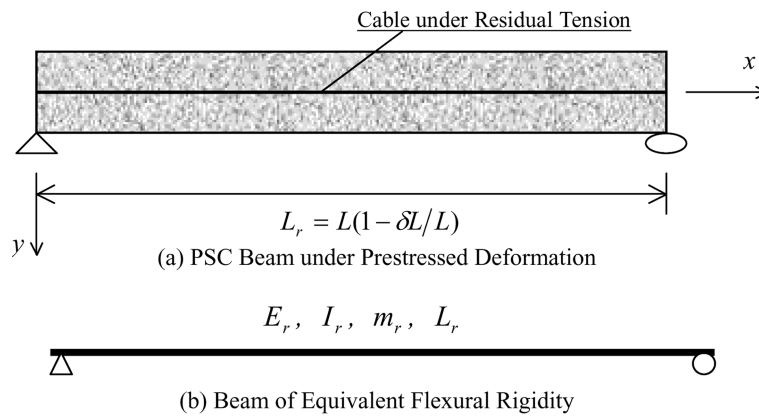


Fig. 2 Equivalent flexural rigidity model of PSC beam (Kim, et al. 2003b)

As an inverse solution of Eq. (9), prestress forces can be identified as:

$$(N)_n = \omega_n^2 m_r \left(\frac{L_r}{n\pi} \right)^2 - E_c I_c \left(\frac{n\pi}{L_r} \right)^2 \quad (10)$$

By assuming no change occurs in beam's geometry and mass properties due to the change in prestress forces, the first variation of the prestress force can be derived as:

$$(\delta N)_n \cong \delta \omega_n^2 m_r \left(\frac{L_r}{n\pi} \right)^2 - \delta(E_c I_c) \left(\frac{n\pi}{L_r} \right)^2 \quad (11)$$

where, $(\delta N)_n$ is the change in prestress force that can be identified by the n th mode; $\delta \omega_n$ is the variation in n th natural frequency due to the prestress-loss; and $\delta(E_c I_c)$ is the change in flexural rigidity of concrete beam section. By relating Eq. (10) to Eq. (11), the relative change in prestress force, which identified from the n th mode, is obtained as (Kim, *et al.* 2003b):

$$\left(\frac{\delta N}{N} \right)_n = \frac{\delta \omega_n^2 - \frac{\delta(E_c I_c)}{m_r} \left(\frac{n\pi}{L_r} \right)^4}{\omega_n^2 - \frac{E_c I_c}{m_r} \left(\frac{n\pi}{L_r} \right)^4} = \frac{\delta \omega_n^2 - \delta \varpi_n^2}{\omega_n^2 - \varpi_n^2} \quad (12)$$

where ϖ_n is the n th natural frequency of the beam with zero prestress force and $\delta \varpi_n$ is the variation in ϖ_n due to $\delta(E_c I_c)$. From Eq. (12), the relative change in prestress force, $\delta N/N$, can be estimated by measuring the change in natural frequencies of the PSC beam. Eq. (12) can be simplified by further assuming no change in concrete flexural rigidity occurred due to the prestress-loss, i.e., $\delta \varpi_n \approx 0$. That is, the prestress-loss can be predicted from natural frequencies of the beam before and after prestress-loss (i.e. $\delta \omega_n^2$, ω_n^2) and natural frequencies of the beam with zero prestress force (i.e. ϖ_n^2).

3. Experimental verification

3.1. Test structure and experimental setup

The schematic of the test structure is shown in Fig. 3. The tested girder spans 6.0 m and installed on testing frame. Its both ends are simply supported by thin rubber pads. The T-beam section girder was reinforced longitudinally and in transverse direction with reinforcing bars with nominal 10 mm diameter (equivalent to Grade 60). The stirrups were used to facilitate the positioning of the top bars. A seven-wire straight concentric monostrand with nominal 15.2 mm-diameter (equivalent to Grade 250) was used as the prestressing tendon. The tendon was placed in a 25 mm-diameter duct that remained ungrouted. The concrete was made of normal Portland cement and had the maximum aggregate size of 25 mm. The 28-day compressive strength of concrete was 23.6 MPa and the mass density was about 2400 kg/m³.

As shown in Fig. 4, the structure was tested in a lab (Smart Structure engineering Lab) located at Pukyong National University, Busan, Korea. A series of tests were performed on the PSC girder from 23 to 25 January, 2007. The lab was air-conditioned to keep temperature and humidity close to constant during the tests. Room-air temperatures ranged from 20.4 °C to 21.5 °C. Temperatures of the PSC girder had little variation as follows: the top surface 18.1~19.3 °C, the middle web surface 17.6~18.7 °C, and the bottom surface 17.0~18.2 °C, which were measured by using K-type thermocouple wires and PXI-4351

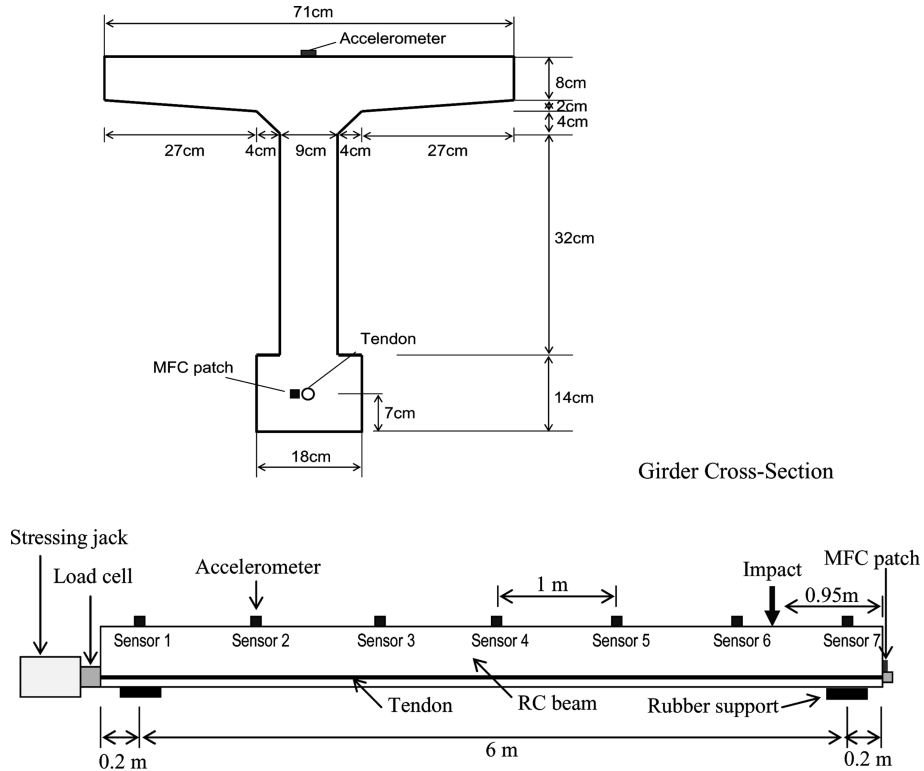


Fig. 3 Schematic of prestressed concrete girder

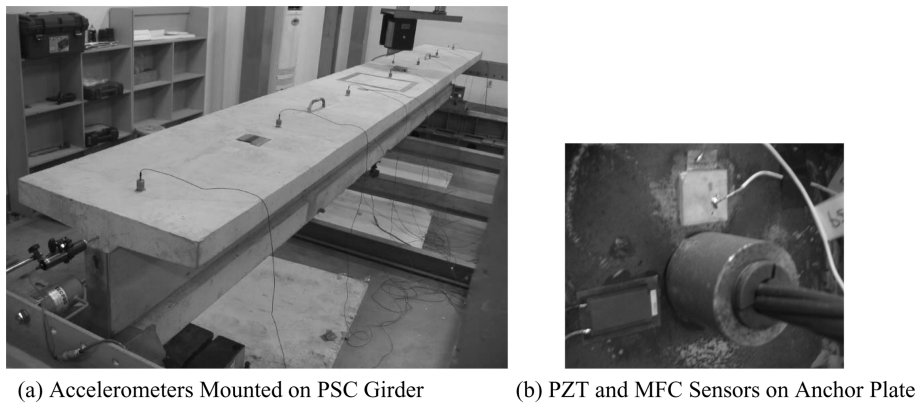


Fig. 4 Experimental setup in PSC girder

Temperature Logger. Temperature effect should be considered when the temperature change leads to significant change in dynamic characteristics. In this study, however, the temperature change was small enough to ignore the temperature effect (Park, *et al.* 1999, Koo, *et al.* 2007, Kim, *et al.* 2007).

Locations and arrangements of sensors on the test structure were designed as shown in Fig. 3. For acceleration measurement, seven sensors (Sensors 1-7) were placed along the girder with constant intervals and the impact excitation was applied at a location 0.95 m distanced from the right edge. A type

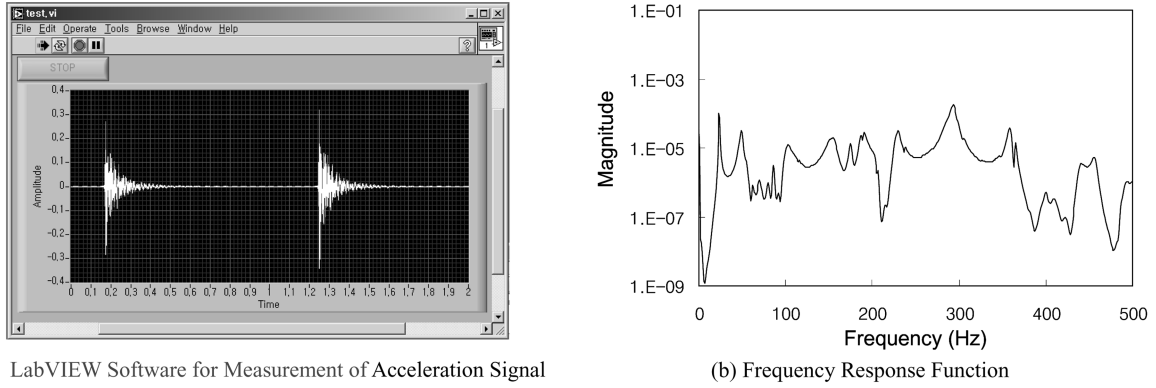


Fig. 5 Acceleration signal and frequency response function of PSC girder

of ICP accelerometers were used in the test: PCB 393B04 with a nominal sensitivity of 1V/g and a specified frequency range ($\pm 5\%$) of 0.06~450 Hz. The accelerometers were connected to the magnetic blocks which were attached to steel washers bonded on the top surface of the girder.

Impact forces, which were not controlled nor recorded, were applied to the PSC girder by dropping a 3 kg-weight hammer. Then dynamic responses in vertical direction were measured at the 7 Stations with a sampling frequency of 1 kHz. It was always positioned on Sensor 3 as the reference channel. A frequency response function obtained from Sensor 3 was used as the reference to calculate frequency-response-ratio, as described in Eq. (3). The data acquisition system included a 16-channels PXI-4472 DAQ, a PXI-8186 Controller, and a PC with LabVIEW and MATLAB. It was set up to acquire signals from the accelerometers and furthermore to extract frequency response functions and modal parameters by frequency-domain decomposition (FDD) technique (Brinker, *et al.* 2001, Yi and Yun 2004). As shown in Fig. 5, acceleration signals were measured from the PSC girder and frequency response functions were extracted by using the FDD method. As shown in Fig. 6, mode shapes of the first four modes were extracted from the acceleration signals measured from the seven accelerometers.

For impedance measurement, a sensor was placed on the anchor plate of the tendon, as shown in Figs. 3 and 4. A type of piezoceramic fiber composite sensor was used: Macro-Fiber Composite (MFC) with the

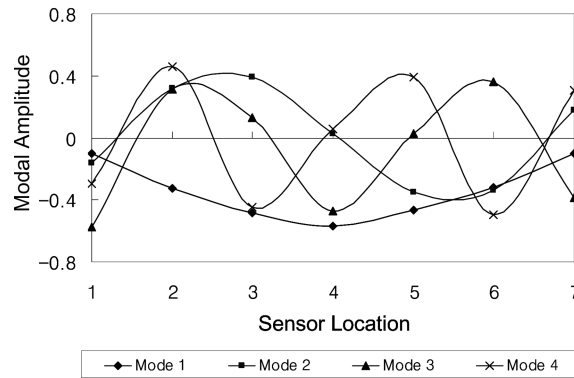


Fig. 6 Mode shapes extracted from acceleration signals

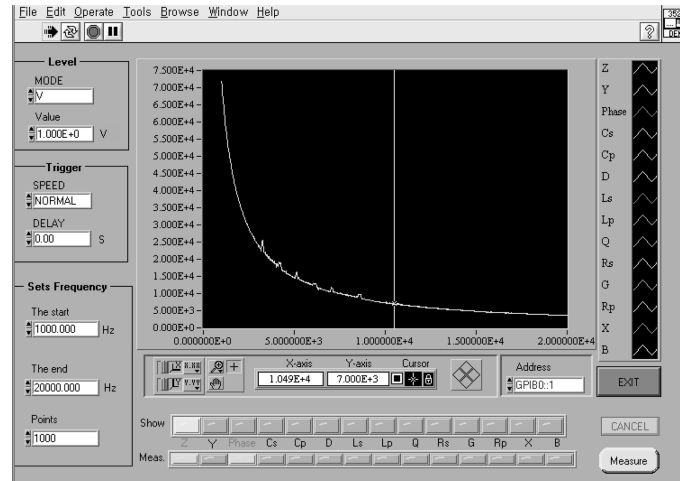


Fig. 7 LabVIEW software for measurement of impedance signatures from anchor plate

size $25.4 \times 12.7 \times 0.254$ mm and the Young's modulus 15 GPa. MFC patches are relatively new type of piezoceramic sensors that are more flexible and less affected by bonding defects than ordinary PZT patches (Park, *et al.* 2006b). A MFC patch was bonded to the surface of the anchor plate near the jacking area. The data acquisition system included an impedance analyzer HIOKI 3532 and a PC with LabVIEW software. With the input voltage of 1 Volt, it was set up to acquire self-diagnosis signals from the MFC sensor and furthermore to extract frequency-domain impedance signatures of real parts. Fig. 7 shows the set-up of LabVIEW software to measure the impedance signals from anchor plate of PSC girder.

Axial prestress forces were introduced into the tendon by a stressing jack as the tendon was anchored at one end and pulled out at the other. A load cell was installed at the left end to measure the applied prestress force. Each test was conducted after the desired prestress force has been applied and the cable has been anchored. During the measurement, the stressing jack was removed from the structure to avoid the effect of the jack weight on dynamic characteristics of the test structure. The prestress forces were applied to the test structure up to five different prestress levels (i.e. PS 1 – PS 5) as summarized in Table 1 and Table 2. There were four prestress-loss cases between the five prestress levels. The maximum and minimum prestress levels were set to 117.6 kN and 39.2 kN, respectively. For each prestress-loss case, the prestress force was uniformly decreased by 19.6 kN.

Table 1 Impedance signatures measured for five prestress levels of PSC girder

Prestress Case	Prestress Force (kN)	Peak Frequency (kHz)	Frequency Shift Index (%)	RMSD damage Index (%)
PS 1	117.6	928.84	-	-
PS 2	98.0	931.09	0.24	3.69
PS 3	78.4	932.08	0.35	5.74
PS 4	58.8	933.33	0.48	6.28
PS 5	39.2	935.58	0.73	9.41

Table 2 Natural frequencies measured for five prestress levels

Prestress Case	Prestress Force (kN)	Natural Frequency (Hz)			
		Mode 1	Mode 2	Mode 3	Mode 4
No Prestress	0	22.73	98.42	218.80	280.74
PS 1	117.6	23.72	102.54	228.87	294.32
PS 2	98.0	23.60	101.70	227.16	291.92
PS 3	78.4	23.39	101.65	225.93	288.54
PS 4	58.8	23.23	101.39	224.20	287.59
PS 5	39.2	23.08	98.73	221.76	284.09

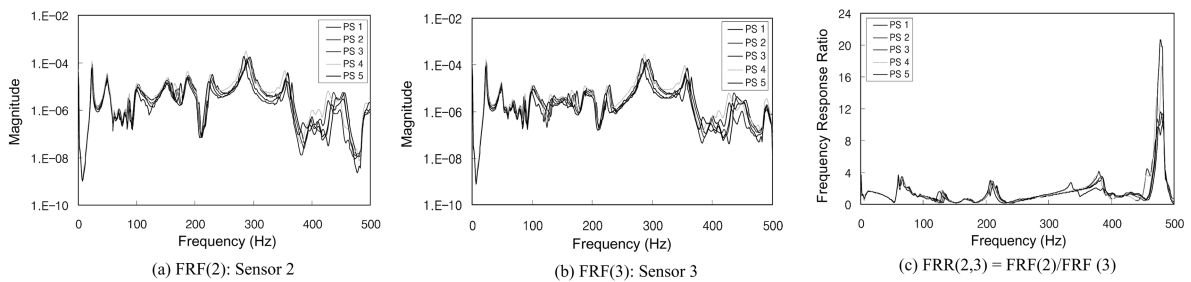


Fig. 8 Frequency response functions for five prestress levels (PS1-PS5)

3.2. Damage occurrence alarming by frequency responses

The occurrence of damage was alarmed in global manner by using the *FRRAC* described in Eq. (4). For each of the five prestress levels, acceleration signals were measured up to eight ensembles from Sensors 2 and 3, which are closely spaced as shown in Fig. 4. (Note that the choice of optimal sensor locations is a research issue that will be examined for a separate study.) As shown in Fig. 8, the frequency-response-ratio function *FRR(2,3)* was obtained from *FRF(2)* and *FRF(3)* measured from Sensors 2 and 3. It is observed from the figure that both *FRFs* and *FRRs* were shifted due to the change in prestress levels. By setting the maximum prestress level, PS 1, as the undamaged baseline state, *FRRAC* values between the reference PS 1 and four other prestress levels (i.e. PS 2 – PS 4) were computed as shown in Fig. 9. The *FRRAC* values were decreased from the unity as the prestress-loss occurred. (Note that we measured eight

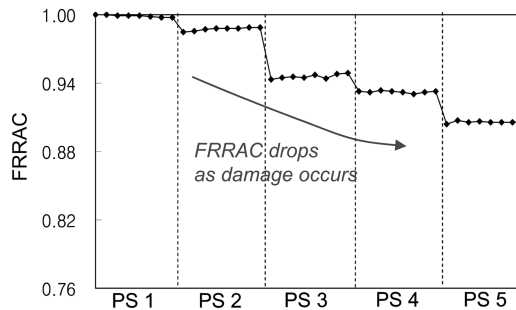


Fig. 9 Global damage alarming of prestress-loss occurrence

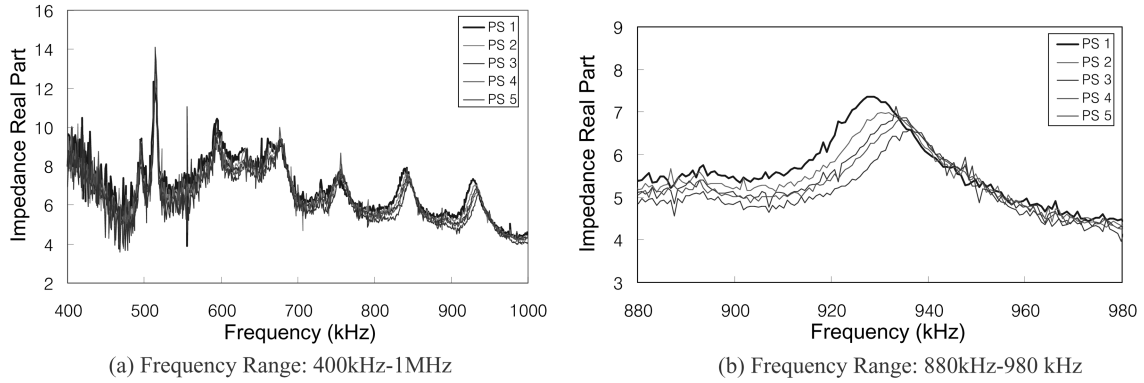


Fig. 10 Impedance signatures for five prestress levels (PS1-PS5)

consecutive *FRRAC* values corresponding to eight ensembles of acceleration signals for each prestress level.) The damages were successfully alarmed for all prestress-loss cases.

3.3. Prestress-loss identification by impedance signatures

The alarmed damage was identified as prestress-loss in PSC girder by using the change in impedance signatures obtained from the experiments. As shown in Fig. 10, impedance real-part signals were measured from the MFC patch for the five prestress levels. Peak frequencies are outlined in Table 1. The frequency range was determined by trial-and-error for impedance signature (Yang, *et al.* 2008, Park, *et al.* 2006). In this study, the impedance signature was examined in a broader frequency range, as shown in Fig. 10(a). A wide frequency range of 400 kHz to 1MHz was first selected and then divided into several partial frequency ranges to choose a suitable frequency range. It was then identified that frequency range 880 to 980 kHz was most sensitive to the prestress-loss, as shown in Fig. 10(b). Also, the changes in impedance signatures were quantified by ‘frequency-shift index’ and ‘root-mean-square-deviation (RMSD) index’. As outlined in Table 1, both frequency-shifts and RMSD indices obviously indicated that the alarmed damage was due to prestress-loss.

3.4. Prestress-loss estimation using modal parameters

The identified prestress-loss damage was estimated in detail. By implementing the prestress-loss prediction model (as described in Eq. (12)), the amount of the prestress-loss was calculated for each vibration mode. From acceleration measurements, natural frequencies of the first four vibration modes were extracted for the five prestress-loss levels, as summarized in Table 2. The corresponding mode shapes were measured as shown in Fig. 6.

As outlined in Table 3, four prediction results were made for four individual modes. As shown in Fig. 11, the predicted prestress-losses of all five prestress cases were compared to the inflicted ones. Except the result by mode 2, the correlations between the inflicted and predicted sets were relatively high and it means that the prestress-loss in the PSC girder could be detected via monitoring changes in natural frequencies. As shown in Fig. 12, the prediction results obtained by averaging all four modes show relatively good matches with the inflicted ones. The prestress-loss estimation errors were 0%~14% for the five prestress cases.

Table 3 Prestress-loss prediction in PSC girder

Prestress Case	Experiment		Prediction Prestress-Loss Results by 4 Modes				Average $\delta N/N$
	N (kN)	$\delta N/N$	Mode 1 $(\delta N/N)_1$	Mode 2 $(\delta N/N)_2$	Mode 3 $(\delta N/N)_3$	Mode 4 $(\delta N/N)_4$	
PS 1	117.6	-	-	-	-	-	-
PS 2	98.0	0.17	0.12	0.21	0.17	0.18	0.17
PS 3	78.4	0.33	0.34	0.22	0.30	0.43	0.32
PS 4	58.8	0.50	0.50	0.28	0.47	0.50	0.44
PS 5	39.2	0.67	0.65	0.92	0.71	0.76	0.76

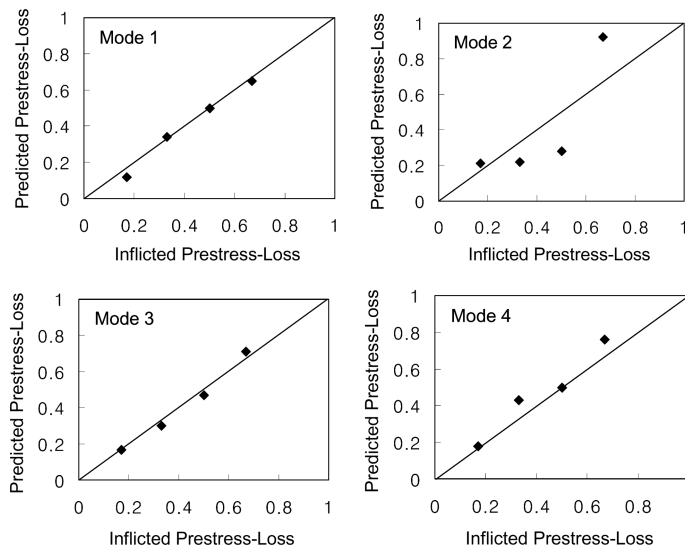


Fig. 11 Correlation between inflicted and predicted prestress-loss results

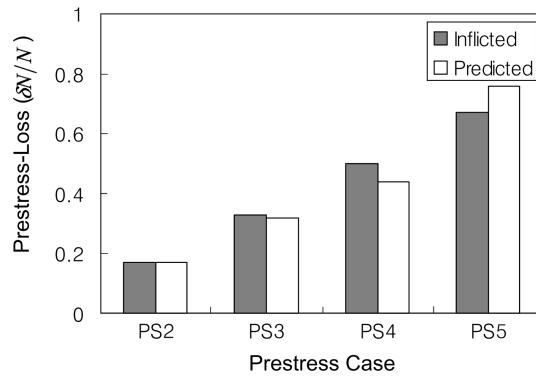


Fig. 12 Prestress-loss estimation results of PSC girder

4. Summary and conclusions

In this paper, a vibration-impedance based monitoring system was newly proposed to predict the loss of prestress forces in prestressed concrete (PSC) girder bridges. Firstly, a global damage alarming algorithm using the change in frequency responses was newly proposed to monitor the occurrence of damage in PSC

girders. Secondly, a local damage detection algorithm using the change in electro-mechanical impedance features was selected to identify the prestress-loss in tendon and anchoring members. Thirdly, a prestress-loss prediction algorithm using the change in natural frequencies was selected to estimate the extent of prestress-loss in PSC girders. Finally, the feasibility of the proposed method was experimentally evaluated on a scaled PSC girder model for which acceleration responses and electro-mechanical impedances were measured for several damage scenarios of prestress-loss.

Total five prestress-loss cases were simulated on the PSC girder. The occurrence of damage was successfully alarmed by measuring the change in frequency responses from accelerometers mounted on the PSC girder. Once alarmed, the damage was successfully identified as prestress-loss by measuring the change in impedance signatures from MFC patches bonded on the prestressing anchor plate. Also, the extent of damage was estimated with relatively good accuracy by using the change in modal parameters of the first four modes. Future studies are remained to assess the effect of modeling errors and environment-induced uncertainties on the feasibility and practicality of the method.

Acknowledgement

This study was supported by Korean Science and Engineering Foundation (KOSEF) through Smart Infra-Structure Technology Center (SISTeC) in the program year of 2005 and Port Remodeling Project under Ministry of Land, Transport and Maritime Affairs in 2008.

References

- Adams, R. D., Cawley, P., Pye, C. J. and Stone, B. J. (1978), "A vibration technique for non-destructively assessing the integrity of structures", *J. Mech. Eng. Sci.*, **20**, 93-100.
- Bendat, J. S. and Piersol, A. G. (1993), *Engineering Applications of Correlation and Spectral Analysis*, Wiley, USA.
- Bhalla, S. and Soh, C. K. (2003), "Structural impedance based damage diagnosis by piezo-transducers", *Earthq. Eng. Struct. Dyn.*, **32**(12), 1897-1916.
- Brinker, R., Zhang, L. and Andersen, P. (2001), "Modal identification of output-only systems using frequency domain decomposition", *Smart Mater. Struct.*, **10**, 441-445.
- Doebling, S. W., Farrar, C. R. and Prime, M. B. (1998), "A summary review of vibration-based damage identification methods", *The Shock Vib. Digest*, **30**(2), 91-105.
- Elsener, B. (2005), "Long-term monitoring of electrically isolated post-tensioning tendons", *Struct. Concrete*, **6**(3), 101-106.
- Giurgiutiu, V. and Zagari, A. N. (2005), "Damage detection in thin plates and aerospace structures with the electro-mechanical impedance method", *Struct. Health Monitor.*, **4**(2), 99-118.
- Kabeya, K. (1998), "Structural health monitoring using multiple piezoelectric sensors and actuators", Master's thesis, Virginia Polytechnic Institute and State University.
- Kim, J. T. and Stubbs, N. (1995), "Improved damage identification method based on modal information", *J. Sound. Vib.*, **259**(1), 57-67.
- Kim, J. T., Park, J. H. and Lee, B. J. (2007), "Vibration-based damage monitoring in model plate-girder bridges under uncertain temperature conditions", *Eng. Struct.*, **29**(7), 263-280.
- Kim, J. T., Ryu, Y. S., Cho, H. M. and Stubbs, N. (2003a), "Damage identification in beam-type structures: frequency-based method vs mode-shape-based method", *Eng. Struct.*, **25**, 57-67.
- Kim, J. T., Yun, C. B., Ryu, Y. S. and Cho, H. M. (2003b), "Identification of prestress-loss in PSC beams using modal information", *Struct. Eng. Mech.*, **17**(3-4), 467-482.
- Kim, J. T., Na, W. B., Park, J. H. and Hong, D. S. (2006), "Hybrid health monitoring of structural joints using

- modal parameters and EMI signatures”, *Proceedings of SPIE*, 6174, 61742O.
- Koo, K. Y., Park, S., Lee, J. J., Yun, C. B. and Inman, D. J. (2007), “Impedance-based structural health monitoring considering temperature effects”, *Proceedings of SPIE*, 6532, 65320C.
- Law, S. S. and Lu, J. R. (2005), “Time domain responses of a prestressed beam and prestress identification”, *J. Sound Vib.*, **288**(4-5), 1011-1025.
- Liang, C., Sun, F. P. and Rogers, C. A. (1994), “Coupled electromechanical analysis of adaptive material systems-determination of the actuator power consumption and system energy transfer”, *J. Intell. Mater. Sys. Struct.*, **5**(1), 12-20.
- Liang, C., Sun, F. P. and Rogers, C. A. (1996), “Electro-mechanical impedance modeling of active material systems”, *Smart Mater. Struct.*, **5**(1), 171-186.
- Lin, T. Y. (1963), *Design of Prestressed Concrete Structures*, John Wiley & Sons, USA.
- Miyamoto, A., Tei, K., Nakamura, H. and Bull, J. W. (2000), “Behavior of prestressed beam strengthened with external tendons”, *J. Struct. Eng.*, **126**, 1033-1044.
- Nawy, E.G (1996), *Prestress Concrete - A Fundamental Approach*, Prentice Hall, USA.
- Park, G., Cudney, H. and Inman, D. J. (2000), “Impedance-based health monitoring of civil structural components”, *J. Infrastruct. Sys.*, ASCE, **6**(4), 153-160.
- Park, G., Farrar, C. R. and Scalea, F. L. (2006a), “Performance assessment and validation of piezoelectric active-sensors in structural health monitoring”, *Smart Mater. Struct.*, **15**(6), 1673-1683.
- Park, G., Kabeya, K., Cudney, H. H. and Inman, D. J. (1999), “Impedance-based structural health monitoring for temperature varying applications”, *JSME Int. J.*, **42**, 249-258.
- Park, S., Ahmad, S., Yun, C. B. and Roh, Y. (2006b), “Multiple crack detection of concrete structures using impedance-based structural health monitoring techniques”, *Experimental Mech.*, **46**(5), 609-618.
- Saiidi, M., Douglas, B. and Feng, S. (1994), “Prestress force effect on vibration frequency of concrete bridges”, *J. Struct. Eng.*, **120**, 2233-2241.
- Saiidi, M., Shield, J., O’connor, D. and Jutchens, E. (1996), “Variation of prestress force in a prestressed concrete bridge during the first 30 months”, *PCI J.*, **41**, 66-72.
- Stubbs, N. and Osegueda, R. (1990), “Global nondestructive damage evaluation in solids”, *Int. J. Analytical Experimental Modal Analysis*, **5**(2), 67-79.
- Yang, Y., Xu, J. and Soh, C. K. (2005), “Generic impedance-based model for structure-piezoceramic interacting system”, *J. Aerospace Eng.*, ASCE, **18**(2), 93-101.
- Yang, Y. W., Hu, Y. H. and Lu, Y. (2008), “Sensitivity of PZT impedance sensors for damage detection of concrete structures”, *Sensors*, **8**(1), 327-346.
- Yi, J. H. and Yun, C. B. (2004), “Comparative study on modal identification methods using output-only information”, *Struct. Eng. Mech.*, **17**(3-4), 445-446.